Multi element integration technology for thermal hazard simulation calibration based on full-scale automotive climate numerical wind tunnel

Dan Wang[1], Xuelong Liu[1],Liansong Mu[1],Haiyang Wang[1],Ziming Yan[1]
1.China Automotive Technology and Research Center Co., Ltd.

wangdan@catarc.ac.cn

liuxuelong@catarc.ac.cn

Abstract: With the rapid development of the automotive industry, the optimization of automotive thermal management systems is crucial for improving overall vehicle performance, safety, and reliability. This article focuses on the multi-dimensional integration technology in the full-scale automotive climate numerical wind tunnel, and elaborates on how to use this technology to accurately simulate and calibrate automotive thermal hazards. By constructing an accurate heat damage simulation model and combining it with the real working conditions simulated in wind tunnels, the heat damage situation of automobiles in different environments is simulated and analyzed, and strict calibration verification is carried out based on experimental data. The research results indicate that the multi-dimensional integration technology based on full-scale automotive climate numerical wind tunnel can effectively improve the accuracy of thermal hazard simulation, provide strong support for the optimization design of automotive thermal management systems, and help the automotive industry make further breakthroughs in energy conservation, emission reduction, and improving driving comfort.

This article delves into the difficult problem of automatic calibration for full-scale automotive climate numerical wind tunnel thermal damage simulation. The vehicle thermal management simulation model for automobiles contains a large number of parameters, and accurate numerical values are difficult to obtain. Parameter calibration is crucial. Therefore, this article constructs an automated optimization process and adopts a dual track technical path: one is manual calibration based on experimental data comparison and expert experience, and the other is intelligent calibration with the help of multiple technical means. At the key technical level, a parametric simulation process is built through graphical software, integrating multiple DOE algorithms, conducting sensitivity analysis, clarifying the sensitivity ranking of input parameters,

Contribution: 2025 FKFS Conference on Vehicle Aerodynamics and Thermal Management
15 – 16 October 2025 | Leinfelden-Echterdingen

and using artificial intelligence algorithms to generate and train proxy models, significantly reducing simulation computation time. The above method ensures that the temperature error between the simulation model and the corresponding position of the test measurement point is controlled within an acceptable engineering range of 5% under the premise of accurately loading the simulation boundary conditions, significantly improving the accuracy and reliability of the simulation results of automotive thermal management and greatly enhancing the calibration efficiency.

1 Introduction

1.1 Research background and significance

In the actual operation of automobiles, heat damage seriously affects the performance, reliability, and service life of vehicles[1-3]. When a car is in motion, components such as the engine and exhaust pipe generate a large amount of heat. If they are not dissipated in a timely and effective manner, it can lead to high temperatures in the components, causing a series of problems such as increased wear and tear, decreased lubricating oil performance, electronic component failure, and even endangering driving safety[4-6]. In addition, in high temperature environments, the driving comfort inside the car will also be greatly reduced. Therefore, it is of great practical significance to conduct in-depth research on the problem of automobile heat damage and seek effective solutions.

Traditional research methods for automobile heat damage often rely on actual vehicle testing. However, actual vehicle testing is not only expensive and time-consuming, but also limited by environmental conditions, testing sites, and other factors, making it difficult to comprehensively and systematically study heat damage issues under various working conditions[7,8]. The emergence of full-scale automotive climate numerical wind tunnels has brought new opportunities for the study of automotive thermal hazards. It can simulate various complex climate conditions and driving conditions, and through multi-dimensional integration technology, couple and analyze multiple physical fields, providing a more realistic and accurate simulation environment for automobile heat damage simulation, which helps to deeply understand the mechanism of heat damage and provide scientific basis for the optimization design of automobile thermal management systems[9-11].

1.2 Current research status at home and abroad

In the field of automotive heat damage research, foreign research started early and achieved fruitful results. Developed countries in the automotive industry, such as Europe, America, and Japan, are leading in thermal damage testing and simulation with advanced full-scale automotive climate wind tunnel laboratories and numerical wind tunnel simulation models[12,13].Mercedes Benz conducted research on engine compartment heat damage under different climatic conditions through numerical simulation technology, optimized the layout of heat dissipation channels, and reduced the high-temperature failure rate of engines by 18%. BMW Group utilizes wind tunnel testing and finite element method to simulate the thermal degradation process of the braking system. By improving the material and structural design of the brake disc, the high-temperature stability of the braking system has been effectively enhanced[14].In the research of simulation algorithms, Stanford University in the United States proposed an improved finite volume method, which increases the computational efficiency of fluid solid coupling by 30%, significantly enhancing the real-time and accuracy of thermal damage simulation[15].

Although the research on automobile heat damage started relatively late in China, it has developed rapidly. The Shanghai Ground Transportation Wind Tunnel Center relies on advanced wind tunnel equipment to conduct research on thermal flow problems in automotive engine compartments[16].The Automotive Wind Tunnel Laboratory of China Automotive Center conducted in-depth analysis of the flow field in the pure motor compartment through a combination of experiments and simulations, and optimized the matching design of the cooling fan and radiator[17].In terms of research institutions, Tsinghua University has made progress in handling boundary conditions for thermal hazard simulation, proposing a dynamic boundary setting method based on actual road conditions, which has improved the fit between simulation results and real vehicle road tests[18].Despite numerous achievements in domestic and international research, there are still significant pain points. Firstly, the deep application of multivariate integration technology in thermal hazard simulation is insufficient. Existing research mainly focuses on single physical fields or simple coupling analysis, and the simulation accuracy of multi physical field coupling effects such as fluid, heat transfer, and thermal radiation under complex working conditions is limited. Secondly, the accuracy and universality of simulation model parameters are poor, with significant differences in material characteristics among different vehicle models and components. Existing model parameters are difficult to adapt to diverse scenarios, resulting in simulation result errors generally exceeding 15%. Thirdly, the collaborative calibration efficiency between experiments and simulations is low, traditional wind tunnel test data acquisition and processing take a long time, and simulation model parameter adjustment relies on empirical trial and error, which cannot meet the rapid iteration requirements of automotive research and development.

2 Full scale automotive climate numerical wind tunnel test

2.1 Structure and Function of Full Scale Automotive Climate Numerical Wind Tunnel

The full-size automotive climate wind tunnel is a large-scale testing facility that can simulate the real driving environment of automobiles. Its structure mainly includes the tunnel body, driving system, measurement and control system, and climate simulation system. The tunnel body is the core part of a wind tunnel, usually adopting a closed or semi closed structure, with sufficient internal space to accommodate a complete car for testing. The driving system uses a powerful motor to drive the fan, generating stable and controllable airflow, simulating the wind speed during car driving. The measurement and control system is responsible for accurately measuring and controlling parameters such as airflow velocity, temperature, and pressure inside the wind tunnel, ensuring the accuracy and stability of the test conditions. The climate simulation system can simulate various complex climate conditions, such as high and low temperatures, solar radiation, rainfall, snowfall, etc., providing a diverse experimental environment for the study of automobile heat damage[19].The function of the full-size automotive climate wind tunnel is very powerful, which can deeply study the thermal management performance of automobiles under high and low temperature, wind, frost, rain, snow, fog and other climate conditions, as well as cloudy and tunnel environments[20].By installing different sensors and measuring devices in wind tunnels and vehicles, real-time monitoring of temperature changes, airflow distribution, and heat dissipation performance parameters of various components of the car can be achieved, providing rich data support for research on car heat damage. In addition, wind tunnels can also be integrated with other testing equipment, such as road load simulation systems, thermal road simulation systems, etc., to further expand their testing functions and achieve comprehensive simulation of complex automotive operating conditions.

The following figure shows the structure of the horizontal reflux 3/4 opening full-size climate wind tunnel of China Automotive Technology Research Center:

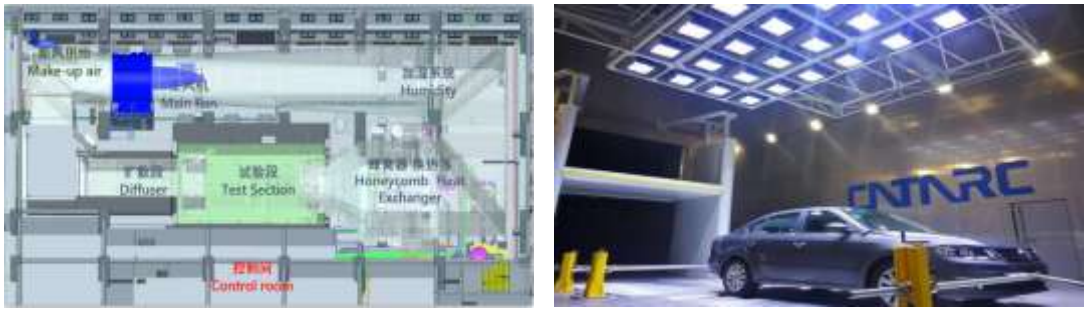

Figure 2.1-1: Climate Wind Tunnel Laboratory of China Automotive Technology Research Center

The various parameter indicators of the wind tunnel are shown in the following table:

Table 2.1.1-1: Climate Wind Tunnel Parameter Indicators

Parameter	Specification
	130 km/h with the large nozzle (13.2 m2 nozzle)

Maximum wind speed	250 km/h with the small nozzle (8.25 m2 nozzle)
Velocity uniformity	1σ(U/Umean) ≤ 0.5% (Small nozzle: X= 1 m, Y=±1.2 m, Z=0.2 m to
Flow angularity	1σ(Δα) ≤ 0.5° 1σ(Δβ) ≤ 0.5° (Small nozzle: X= 1 m, Y=±1. 1 m, Z=0.2 m to
Turbulence Intensity Uniformity	Tu ≤ 0.5 % (f = 20 Hz to 4 kHz) (Small nozzle: X= 1 m, Y=±1.0 m, Z=0.2 m to
Wind speed controllability	Under steady state conditions, the wind speed
Boundary Layer	δ * ≤ 4 mm at X = 1 m
Axial Static Pressure Gradient	dCp/dx ≤ 0.002 m- 1 (X=1 m to 9 m, Y= 0, Z=1 m)
Static Pressure Pulsations	Cprms ≤ 0.02 (X = 7 m, Y = 4.5 m)
Air temperature range	-40ºC to +60ºC
Air temperature uniformity	1σ(T) ≤ 0.5°C
Air temperature	Under steady state conditions, the air temperature
Air temperature transition time limits (at 110 km/h)	+ 10ºC to +45ºC in less than 43.75 minutes +45ºC to +10ºC in less than 43.75 minutes
Humidity range	5% RH to 95% RH (non-condensing, maximum dewpoint = 36.7°C)
Humidity controllability	Under steady state conditions, the humidity shall
Humidity transition time limits	20%RH to 80%RH in 30 minutes at 35ºC 80%RH to 20%RH in 30 minutes at 35ºC
Background Noise Level	80 dB(A) at 100 km/h (measured out-of-flow)

Numerical wind tunnel is a 1:1 reconstruction of a physical wind tunnel, establishing a virtual simulation wind tunnel, reproducing various climate conditions in the physical wind tunnel on a computer, and using CFD methods to obtain low-cost, fast, and accurate thermal performance results of vehicles. Due to the main testing area being located in the chamber, in order to reduce computational costs, the numerical wind tunnel intercepts the flow channels between the chamber and the front and rear corners. The main retained components include the contraction section, evaporator, honeycomb device, chamber, nozzle, boundary layer suction porous plate, sunlight simulation device, chassis dynamometer hub, vehicle fixing device, collection port, and collection section flow channel. As shown in the following figure:

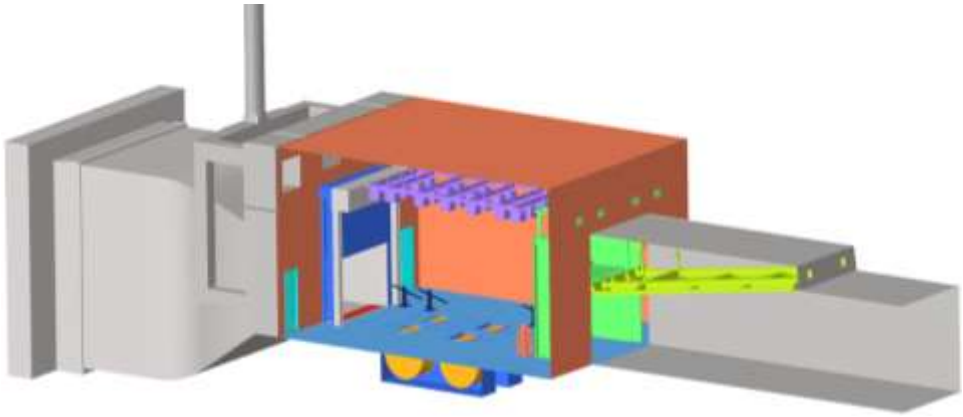

Figure 2.1.3: Climate Numerical Wind Tunnel

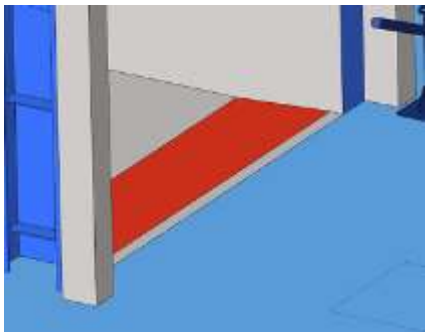

Figure 2.1.4: Boundary layer suction device

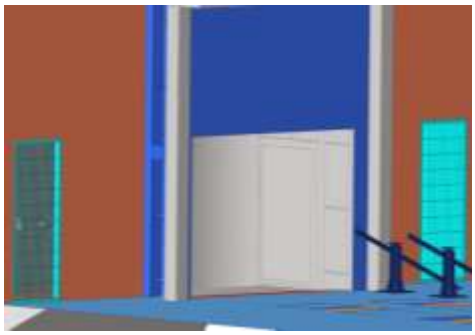

Figure 2.1.5:Adjustable nozzle

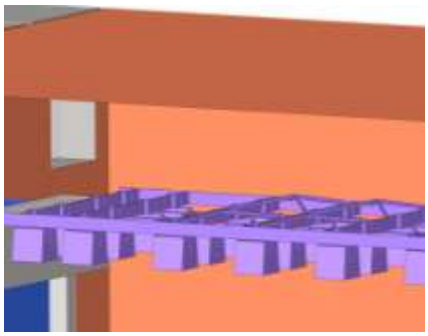

Figure 2.1.6: Sunshine Simulation Device

Figure 2.1.7: Chassis dynamometer hub

2.2 Experimental equipment and instruments

The equipment required for full-scale automotive climate numerical wind tunnel testing mainly includes the wind tunnel body, climate simulation system, measuring instruments, etc. The wind tunnel body provides a stable and controllable airflow environment, and its fan system can generate airflow of different wind speeds to simulate the working conditions of a car at various speeds; The climate simulation system can adjust environmental parameters such as temperature, humidity, and solar radiation intensity inside the wind tunnel to simulate different climate conditions. The parameters of the wind tunnel equipment are shown in the following table:

Table 2.2-1: Parameters of Climate Wind Tunnel Equipment

No.	Equipment	Parameter
1	Master Nozzle	8.25m2
2	Master Nozzle Max. Wind Speed	250km/h
3	Truck Nozzle	13.2m2
4	Truck Nozzle Max. Wind Speed	170km/h
5	Reverse Wind Max. Speed	20km/h
6	Wind Speed Control Tolerance	≤±0.5km/h
7	Vehicle Speed Range	0~250km/h
8	Temperature Range	-40~+60℃
9	Temperature Control Tolerance	≤±0.5 ℃
10	Humidity Range	5~95%
11	Humidity Control Tolerance	≤±3%
12	Solar Simulation Intensity	300~1200W/ m2
13	Other abilities	Hot Road Simulation
		Rain & Snow Simulation

Measuring instruments are used to obtain various physical parameters during the experimental process, mainly including temperature sensors, wind speed sensors, flow sensors, radiation sensors, etc. The temperature sensor uses high-precision thermocouples or platinum resistors to measure the surface temperature of various components of the car, engine coolant temperature, air temperature, etc; Wind speed sensors typically use pitot tubes, cobra probes, or impeller anemometers to measure the airflow velocity distribution inside the wind tunnel and the airflow distribution on the surface of the cooling module. Pressure sensors are used to measure parameters such as high and low pressure in refrigerant systems, tire pressure, etc. Radiation sensors are used to measure the thermal radiation intensity of the car roof, providing boundary inputs and reference targets for thermal hazard analysis. The main focus of this analysis is on the temperature target of vehicle heat damage, using two types of temperature sensors: high temperature and low temperature. The model parameters are shown in the table below:

Table 2.2-2: Temperature Sensor Parameter Table

No.	Model	Lengh(m)	Measuring range(℃)	Temperature resistance limit of cables(℃)
1	Armored K-	5	-200℃~1000℃	-200℃~400℃
2	Type K	5	-50℃~260℃	-50℃~260℃

The temperature measuring points of ordinary thermocouples are rolled into a coil shape and attached to the surface of the object being measured with cloth tape. The cables are fixed at room temperature along the way with tape. Finally, the sensor wire harnesses at similar positions are tied and tied with zip ties, and the other end is connected to the data acquisition instrument. High temperature thermocouples are armored and not easily bent. The measuring point is glued to the surface of the object being measured with iron, and the high-temperature resistant section behind the measuring point is fixed to the nearby pipe section with a metal clamp to ensure the stability of the measuring point during testing. It should be noted that when pasting

measuring points, the beginning and end of each sensor should be uniformly marked with label paper to avoid confusion in measuring point output after multiple cables are tied together. After connecting all measuring points to the data acquisition equipment, open the testing software to check the signal status and ensure that all sensors can output temperature values in a timely and accurate manner. The layout methods of two types of sensors on the vehicle are shown in the following figure:

Figure 2.2-1: Layout of Type K

Figure 2.2-2: Layout of Armored K-type

2.3 Test conditions and results

During the experiment, various physical parameter data were collected in real-time using measuring instruments, and stored and transmitted through a data acquisition system. The temperature data collection frequency is 1HZ. The collected data needs to be preprocessed, including data filtering, outlier removal, and other operations, to improve data quality. Then, use data analysis software to perform statistical analysis on the processed data. By analyzing the experimental data, the temperature distribution information of various components of the car under different working conditions is obtained, providing a basis for the calibration of the thermal damage simulation model. The following table shows the average temperature values of each thermal equilibrium stage after data processing in this experiment. Among them, the ambient temperature, vehicle speed, and surface temperature of the heat source are used as simulation input conditions, and the surface temperature of the target component is the target value calibrated by simulation.

Table 2.3-1: Surface Temperature Values of Heat Sources for Vehicle Thermal Balance Test

No.	Heat source components	Surface measurement point temperature(℃)		
		Medium speed climbing(60kph)	High speed climbing(110kph)	Maximum speed(150kph)
1	Cylinder head	101.23	89.46	85.63
2	Cylinder linder	106.40	93.71	90.23
3	Cylinder block	119.55	102.69	96.00
4	Oil pan	117.81	107.11	104.45

5	Engine side cover	112.93	101.07	98.92
6	exhaust manifold	121.00	110.88	108.07
7	Cold end of	83.38	87.92	91.36
8	Hot end of	639.89	625.19	629.28
9	Pre urging	643.98	611.77	618.88
10	Pre urging	240.39	165.45	139.52
11	Front pipe of	542.29	503.56	502.60
12	Corrugated pipe	213.29	142.09	132.29
13	Main reminder	525.67	487.18	484.15
14	Main reminder	355.96	299.11	287.67
15	Front	434.70	380.29	375.56
16	Front	153.78	111.97	97.86
17	Front	427.97	382.03	384.25
18	Central muffler	180.38	131.76	129.00
19	Front pipeline of	358.76	307.95	306.20
20	Rear muffler	277.37	229.09	227.77
21	Tail pipe	281.44	239.20	271.57

Table 2.3-2:Temperature Table of Target Components for Whole Vehicle Thermal Balance Test

Target component	Surface measurement point temperature(℃)		
	Medium speed climbing(60kph)	High speed climbing(110kph)	Maximum speed(150kph)
Exhaust lifting ear	110	85	80

3 Construction of Automotive Thermal Damage Simulation Model Based on Multivariate Integration Technology

3.1 Modeling and Grid Division

Grid partitioning is one of the key steps in constructing a simulation model for automotive thermal hazards, and the quality of the grid directly affects the accuracy and computational efficiency of the simulation results. In the thermal hazard simulation of full-scale automotive climate numerical wind tunnel, due to the complex structure of the automotive model and the drastic changes in the flow and temperature fields, a mixed grid partitioning method is usually used. For key parts such as the car body and engine compartment, high-precision unstructured hexahedral grids are used for partitioning to accurately capture complex geometric shapes and physical phenomena; For areas far away from cars, use sparser grids to reduce computational complexity. At the same time, boundary layer mesh division is carried out at the interface between fluid and solid, and in areas with large temperature gradients, with local mesh refinement to ensure computational accuracy. In addition, in order to

improve the quality of the grid, it is necessary to perform smoothing treatment on the grid to avoid problems such as distortion and distortion. The following table shows the mesh division parameters of the wind tunnel:

Table 3.1-1: Grid Parameter Setting Table

No.	Project	Parameter
1	Body mesh type	Trimmer
2	Total thickness of boundary layer	2 mm
3	Boundary layers	2层
4	Boundary layer growth rate	1.3
5	Total number of body grids	7674万

The grid division is shown in the following figure:

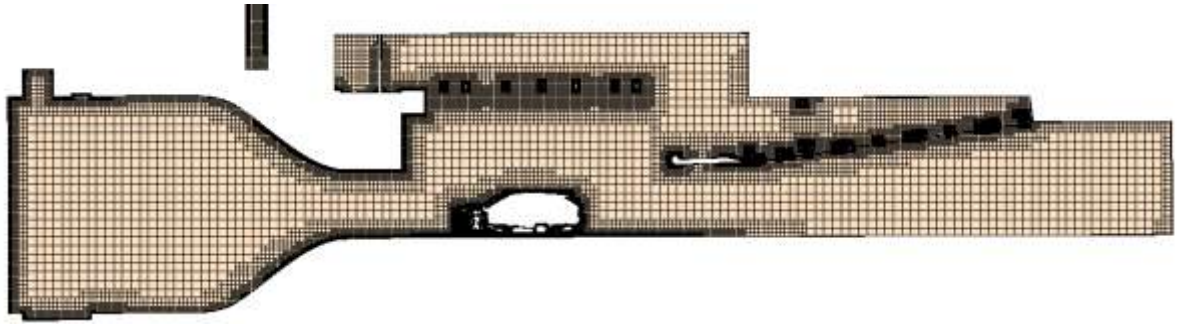

Figure 3.1-1: Longitudinal section mesh of the whole vehicle and wind tunnel

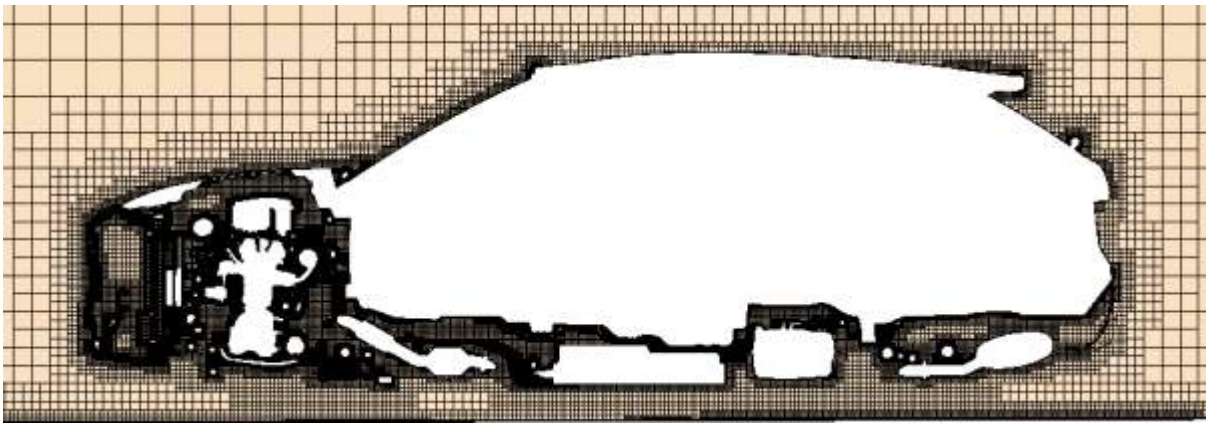

Figure 3.1-2: Vehicle Grid Encryption Zone

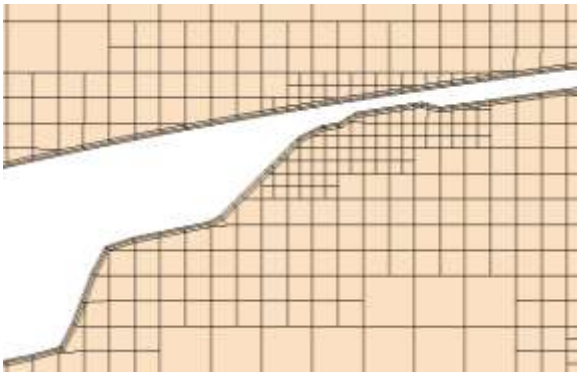

Figure 3.1-3:Grid of Body Surface Layer

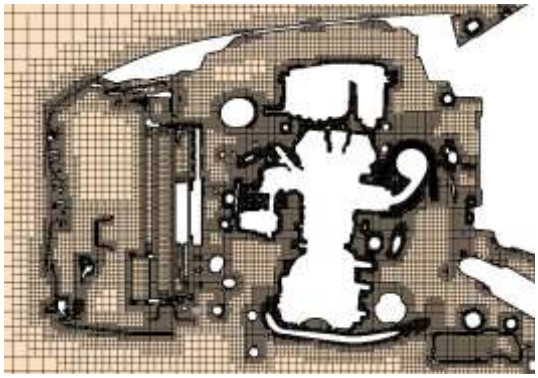

Figure 3.1-4:Engine Compartment Grid

3.2 Boundary condition setting

The accurate setting of boundary conditions is an important prerequisite for ensuring the reliability of simulation results. In the thermal hazard simulation of a full-scale automotive climate numerical wind tunnel, the boundary conditions mainly include the following categories:

- 1. Entrance boundary conditions: Set the air flow velocity and temperature parameters based on the simulated working conditions in the wind tunnel. For the driving conditions of automobiles, the wind tunnel nozzle is usually set as the air flow inlet, with the speed direction opposite to the direction of the car's travel. For simulations of different climate conditions, the temperature and density parameters of the inlet air are adjusted.

- 2. Export boundary conditions: generally set as pressure outlet, with a value of atmospheric pressure. On the premise of ensuring stable calculation, the setting of outlet pressure should be as close as possible to the actual working conditions to avoid problems such as reflux caused by improper outlet pressure setting affecting the calculation results.

- 3. Wall boundary conditions: For solid walls such as car bodies and engine compartment components, non slip boundary conditions are adopted, which means that the air flow velocity at the wall is zero. For heating components such as engines and exhaust pipes, their surface temperature needs to be set according to the test values. In addition, for moving parts such as wheels and cooling fans, a rotating coordinate system is used to simulate the effects of their rotational motion on the surrounding flow field and temperature field.

- 4. Boundary conditions for heat exchangers: Tube fin heat exchangers such as condensers and radiators use air to carry away heat from the fluid medium for heat exchange. In CFD, they are simplified as porous media, with inertial and viscous drag coefficients set, and the gas-liquid heat transfer under vehicle operating conditions set.

The boundary parameters of the entire vehicle are shown in the following table:

Table 3.2-1: Vehicle Boundary Parameter Setting Table

No.	Boundary	Medium speed climbing (60kph)	High speed climbing (110kph)	Maximum speed (150kph)
1	Wind tunnel nozzle airflow	151.5kg/s	277.8kg/s	378.9kg/s
2	Relative export pressure	0 Pa	0 Pa	0 Pa
3	Ambient temperature	38℃	40℃	40℃
4	Air density	1.119kg/m^3	1.110kg/m^3	1.110kg/m^3
5	Wheel speed	431.3rpm	790.7rpm	1078.3rpm
6	Cooling fan speed	2300rpm	2300rpm	2300rpm
7	Hub speed	167.1rpm	306.3rpm	417.7rpm
8	Condenser ventilation resistance inertia coefficient	216.93kg/m^4	216.93kg/m^4	216.93kg/m^4
9	Condenser ventilation resistance viscosity coefficient	685.45kg/m^3-s	685.45kg/m^3-s	685.45kg/m^3-s
10	Ventilation resistance inertia coefficient of radiator	195.39kg/m^4	195.39kg/m^4	195.39kg/m^4
11	Ventilation resistance viscosity coefficient of radiator	595.85kg/m^3-s	595.85kg/m^3-s	595.85kg/m^3-s
12	Condenser heat exchange	7kw	7kw	7kw
13	Heat exchange of radiator	32.7kw	34.5kw	35.9kw

4 Calibration and Verification of Thermal Damage Simulation Model under Dual track Technology

4.1 Manual calibration based on experimental data comparison and expert experience

4.1.1. Calibration method and process

The calibration of the heat damage simulation model is the process of adjusting the model parameters to make the simulation results consistent with the experimental data. The calibration method in this section mainly adopts traditional manual calibration. Firstly, manual parameter screening is conducted based on experience to identify key parameters that have a significant impact on the simulation results of the target, such as the heat source near the target component and the thermal conductivity and emissivity of the target component itself. By changing the values of these key parameters and observing the trend of simulation results, identify the components and parameters that have a significant impact on the simulation results and sort them. Then, within a reasonable range of parameters, arrange and combine calculations until the error between the simulation results and experimental values is within ± 8 ℃, which is considered to meet the standard. The calibration process is shown in the following figure:

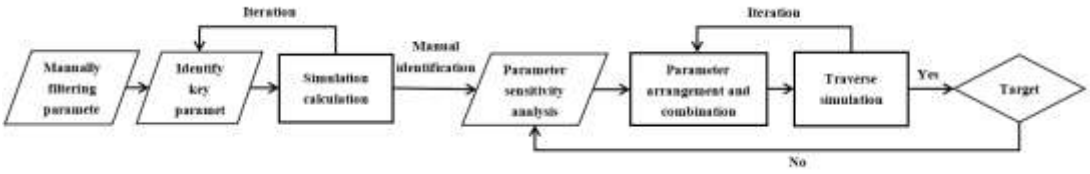

Figure 4.1.1-1: Manual Calibration Process

The target value for this study is the surface temperature of the exhaust hanging ear. Due to its proximity to the exhaust pipe heat source, the thermal emissivity of this pipe section is selected as the key parameter. The hanging ear itself is made of black rubber material, and the thermal emissivity of the hanging ear and the thermal conductivity of the rubber material are also selected as key parameters. Based on simulation experience, heat sources and metal surfaces near the target component may also have an impact on it. Therefore, the thermal emissivity and aluminum material thermal conductivity of the front suspension, chassis, engine, and exhaust pipe surfaces are selected as key parameters. The key parameters of other components are selected using the same method. The thermal emissivity ranges from 0 to 1, the thermal conductivity of rubber materials varies from 0.6 to 1.5, and the thermal conductivity of aluminum materials varies from 225 to 249. The following table shows the key parameters identified manually and their values during preliminary simulation calculations:

Table 4.1.1-1: emissivity Values in Simulation Model

Variable	Front suspension	Floor panel	Engine	Exhaust pipe	Heat Shield	Exhaust lifting ear

Emissi-vity	Base	0.80	0.80	0.80	0.80	0.80	0.80
	Case1	0.95	0.95	0.95	0.95	0.95	0.95
	Case2	0.90	0.90	0.90	0.90	0.90	0.90
	Case3	0.70	0.70	0.70	0.70	0.70	0.70
	Case4	0.60	0.60	0.60	0.60	0.60	0.60
	Case5	0.50	0.50	0.50	0.50	0.50	0.50
	Case6	0.40	0.40	0.40	0.40	0.40	0.40
	Case7	0.30	0.30	0.30	0.30	0.30	0.30
	Case8	0.20	0.20	0.20	0.20	0.20	0.20
	Case9	0.10	0.10	0.10	0.10	0.10	0.10

Table 4.1.1-2: Thermal conductivity values in the simulation model

Variable		Heat Shield	Exhaust lifting ear
Thermal conductivity (W/m-K)	Case10	235.0	0.85
	Case11	233.0	0.80
	Case12	231.0	0.75
	Case13	229.0	0.70
	Case14	227.0	0.65
	Case15	225.0	0.60
	Case16	239.0	1.00
	Case17	241.0	1.10
	Case18	243.0	1.20
	Case19	245.0	1.30
	Case20	247.0	1.40
	Case21	249.0	1.50

After calculating in a full-scale climate numerical wind tunnel, the extracted surface measurement point temperature of the target component is:

Table 4.1.1-3: Simulation Results

CFD result	Temperature measurement point of exhaust suspension ear(℃)		
	Medium speed climbing(60kph)	High speed climbing(110kph)	Maximum speed(150kph)
Base	114.28	89.84	79.32
Case1	118.00	92.99	82.50
Case2	116.91	92.74	81.42
Case3	112.29	87.68	77.35
Case4	109.18	85.53	75.48
Case5	107.24	83.70	73.72
Case6	104.06	82.13	72.14
Case7	101.67	81.19	70.81
Case8	98.60	79.70	69.77
Case9	95.21	78.99	69.02
Case10	114.50	90.03	79.48

Case11	114.72	90.24	79.65
Case12	114.97	90.45	79.84
Case13	116.16	90.41	80.03
Case14	116.47	90.63	80.24
Case15	116.22	90.87	80.47
Case16	114.68	89.48	79.02
Case17	114.28	89.75	78.76
Case18	113.52	88.86	78.51
Case19	112.83	88.44	78.28
Case20	112.84	88.33	78.08
Case21	112.65	87.97	77.88

Comparing the simulation and experimental results, Case 3, Case 4, and Case 5 under medium speed conditions are close to the measured values. Under high-speed conditions, in addition to Case 3, Case 4, and Case 5 approaching the measured values, Case 19 to Case 21 also show a clear trend towards approaching the target temperature. At the highest speed, Case 13 is optimal, and the errors of other cases are also less than 10%. From this, it can be concluded that under low wind speed conditions, the sensitivity of parameters in CFD simulation is ranked from high to low as follows: emissivity>thermal conductivity>convective heat transfer. However, in high wind speed simulations, convective heat transfer becomes more important.

Next, we will arrange and combine the parameter variables from the highly sensitive cases, resulting in a total of 72 sets of parameters and 72 simulation examples. Submit calculations to a 448 core CPU server, taking a total of 288 hours. Select one set of parameters from the 72 sets with an error within 8 ℃ compared to the experimental results, as shown in the table below:

Table 4.1.1-4: Combination of Standard Parameters

Variable		Front suspension	Floor panel	Engine	Exhaust pipe	Heat Shield	Exhaust lifting ear
T-Case 107	Emissivity	0.70	0.60	0.60	0.70	0.30	0.90
	Thermal conductivity(W/m-K)	/				249.0	1.50

4.1.2. Verification method and result analysis

Model validation is an important step in verifying the accuracy and reliability of calibrated simulation models. The verification method mainly adopts comparative analysis to compare the simulation results of the calibrated simulation model under new experimental conditions with the actual experimental data. Select test conditions

different from the calibration conditions, conduct wind tunnel tests, and obtain test data. Then, the calibrated simulation model is used to simulate and calculate the new operating conditions, and the simulation results are compared and analyzed with the experimental data. Evaluate the error between simulation results and experimental data. If the error between the simulation results and the experimental data is within an acceptable range, it indicates that the calibrated simulation model has high accuracy and reliability, and can effectively simulate the problem of automobile heat damage. If the error is large, further analysis of the reasons is needed to check whether there are problems in model construction, parameter settings, experimental data, etc., and re calibrate and verify until the model meets the accuracy requirements.

The same vehicle, same measuring point, and 80kph working condition heat balance experiment were conducted in the same climate wind tunnel. The environmental conditions and heat sources are shown in the following table:

Table 4.1.2-1: Test Environment Conditions

No.	Boundary	Speed 80kph
1	ambient temperature	40℃
2	air density	1.110kg/m^3
3	Cooling fan speed	2300rpm
4	Condenser heat exchange	7kw
5	Heat exchange of radiator	30.2kw

Table 4.1.2-2: Test Heat Source Temperature

No.	Heat source components	Speed 80kph
1	Cylinder head	85.32
2	Cylinder linder	90.40
3	Cylinder block	98.56
4	Oil pan	100.03
5	Engine side cover	87.20
6	exhaust manifold	100.09
7	Cold end of turbocharger	83.50
8	Hot end of turbocharger	621.09
9	Pre urging pipeline	608.70
10	Pre urging	130.39
11	Front pipe of corrugated pipe	497.80
12	Corrugated pipe	150.40
13	Main reminder front pipe	477.59
14	Main reminder	285.06
15	Front consumption front pipe section	369.15
16	Front consumption	100.10
17	Front consumption rear pipe section	380.12
18	Central muffler	150.00
19	Front pipeline of rear muffler	300.87

20	Rear muffler	225.06
21	Tail pipe	233.64

Table 4.1.2-3: Test Target Temperature

Target component temperature(℃)	Speed 80kph
Exhaust lifting ear	74.5

Set the simulation model according to the parameters in Table 4.1.1-4, and obtain the CFD results as shown in the following table:

Table 4.1.2-4: Simulation Results

Target component temperature(℃)	Experimental value	Simulated value	Absolute error	Relative error
Exhaust lifting ear	74.5	69.3	5.2	7%

The result meets the absolute error requirement of less than ± 8 ℃, and the relative error is also within an acceptable range.

However, in actual engineering development, there are 30-60 target components for thermal damage in a vehicle, and key parameters also have mutual influence. Manually calibrating them one by one will consume a lot of manpower, computing power, and time, which is difficult to achieve in tight engineering development. Therefore, it is necessary to find a fast and efficient automatic calibration method to accelerate the progress of vehicle development.

4.2 Intelligent calibration based on multiple technologies

4.2.1. Calibration method and process

The calibration method in this section mainly adopts a combination of parameter sensitivity analysis and optimization algorithms. Firstly, conduct parameter sensitivity analysis to determine the key parameters and their impact coefficients that have a significant impact on the simulation results. Build a response surface model, optimize with experimental data as the objective function, and find parameter combinations with an error of less than 3%. The calibration process is as follows:

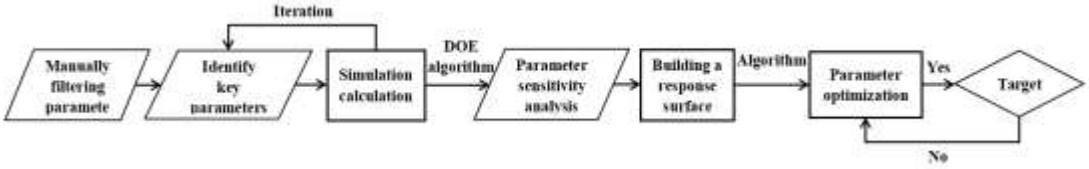

Figure 4.2.1-1: Intelligent Calibration Process

This study aims to simulate and benchmark the surface temperature measurement points of exhaust suspension ears. Select the heat source, heat shield, and its own emissivity and thermal conductivity near the target component as variables. The thermal emissivity ranges from 0 to 1, the thermal conductivity of rubber materials varies from 0.6 to 1.5, the thermal conductivity of stainless steel materials varies from 50 to 80, and the thermal conductivity of aluminum materials varies from 225 to 250.

Using the results of the first round of 66 simulation examples as the initial dataset, a graphical software was called to perform parameter sensitivity analysis. The sorting is shown in the following figure:

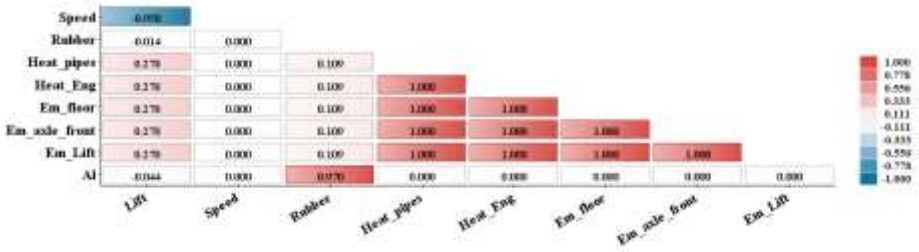

Figure 4.2.1-2: Parameter Sensitivity Statistical Chart

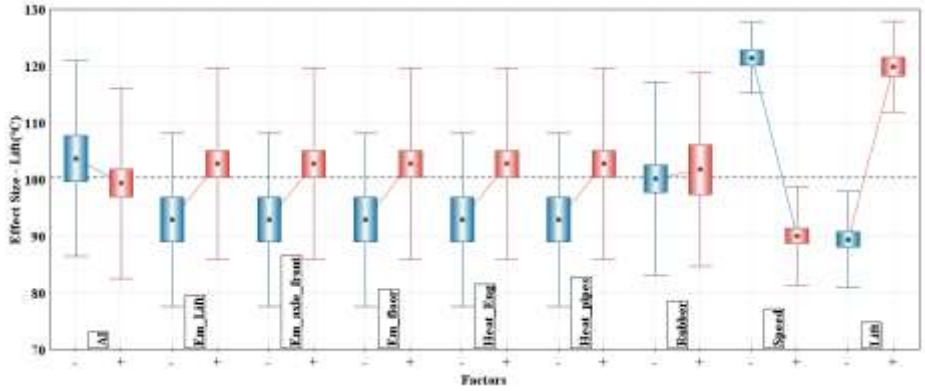

Figure 4.2.1-3: Parameter Sensitivity Box Diagram

In the figure, Speed represents the vehicle speed, Rubber represents the thermal conductivity of the suspension lug rubber material, Heat_pipes represents the emissivity of the exhaust pipe heat source near the suspension lug, Heat_Eng represents the emissivity of the engine heat source near the suspension lug, Em_foor represents the emissivity of the bottom plate, Em_axle_front represents the thermal emissivity of the front suspension, Em_Lift represents the thermal emissivity of the suspension lug, Al represents the thermal conductivity of the exhaust pipe aluminum heat shield, and Lift represents the target temperature on the surface of the suspension lug.

From the parameter sensitivity statistics in Figures 4.2.1-2 and 4.2.1-3, it can be seen that vehicle speed has the greatest impact on the surface temperature of the lifting lug, and the influencing factor is negative. This is because vehicle speed directly affects the convective heat transfer coefficient on the surface of the lifting lug. The higher the vehicle speed, the faster the surface air flow, resulting in faster convective heat transfer. Next are the emissivity of nearby components, the thermal conductivity of the heat shield, and the thermal conductivity of the material of the lifting ear itself.

Data training, due to the consistent dimensions of different temperature measurement points but significant differences in numerical ranges, for example, the surface temperature range of a fan motor is 96 ℃~166 ℃, while the range of a fuel filler tube is 46℃~53℃. This article normalizes the input using Z-score normalization and the output using Z-score normalization to eliminate anisotropy and accelerate network convergence. Both sets of Scalers are serialized and saved to ensure consistency between offline training and online deployment. The use of ensemble learning methods for prediction combines the ability of multi-layer perceptrons (MLPs) to capture nonlinear relationships and complex patterns with the advantages of random forests in handling noisy data. After training the MLP and random forest models separately, use a weighted voting strategy to obtain the final output results.

We first constructed a three-layer feedforward neural network to capture the nonlinear mapping between 8-dimensional temperature characteristics and 4-dimensional thermal properties parameters. The number of hidden layer units is 64 and 32 respectively, and all hidden layers use ReLU activation functions to ensure gradient sparsity and computational efficiency. To suppress overfitting, the model adds a dropout layer after each hidden layer and incorporates L2 weight decay into the loss function. The optimizer uses Adam with an initial learning rate 1×10^{-3}. During the training phase, 10% of the samples are randomly selected from the original training set as the internal validation set, and an early stopping strategy is adopted to avoid overfitting, with a maximum of 500 epochs of training.

Additionally, construct a random forest regressor to utilize its integrated variance reduction and robustness to outlier measurement points. The base learner uses CART regression tree and constructs diversity through self sampling and random subspace strategy. To prevent excessive growth of a single tree, set $\text{max\_depth} = 3$ and $\text{min\_samples\_split} = 2$ for strong regularization.

The optimal number of n_estimators trees within the range of $\{10,20,50,100,200\}$ is determined through grid search using 5-fold cross validation MSE as the evaluation metric, and the final optimal number of trees is 100. This hyperparameter combination performs best in the bias variance trade-off, maintaining sufficient model complexity to capture nonlinear interactions between temperature and thermal properties, while significantly reducing prediction variance through ensemble averaging. Extract the training result data and perform curve fitting, as shown in the following figure:

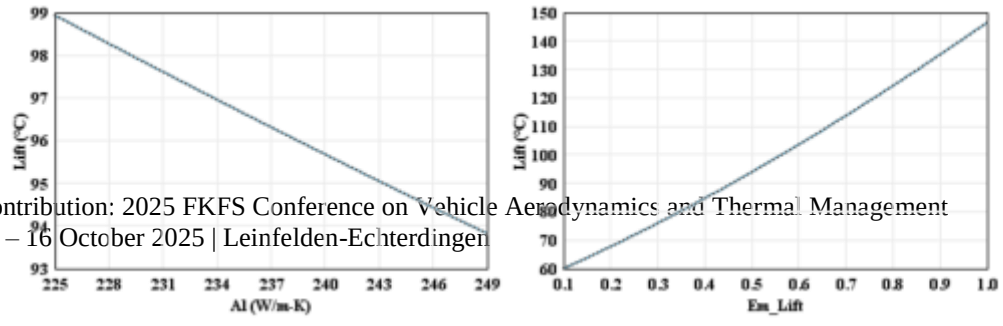

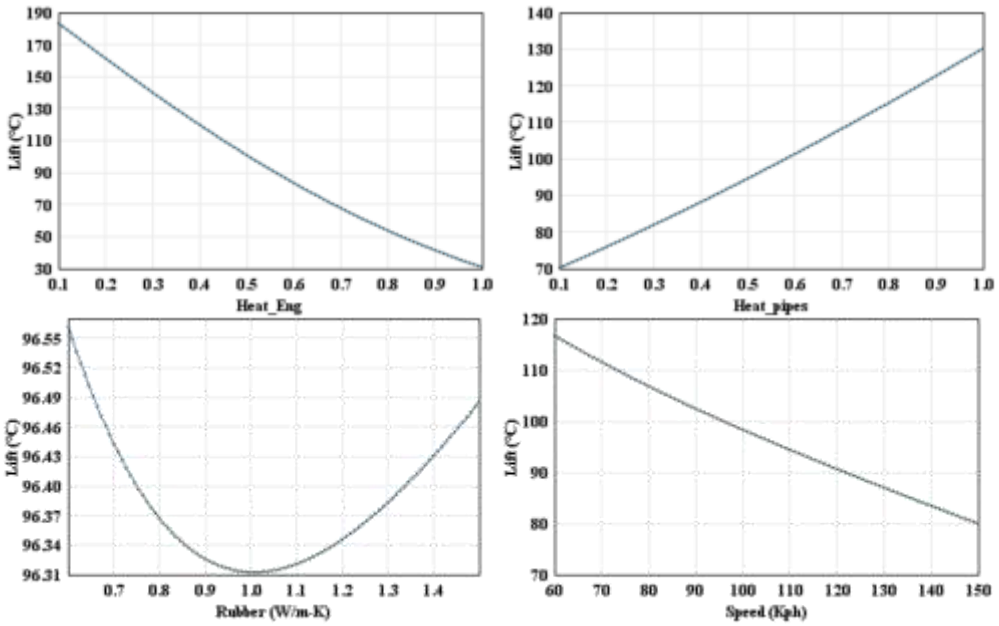

Figure 4.2.1-4: Relationship Curve between Variables and Target Temperature

From Figure 4.2.1-4, it can be seen that the relationship between the thermal conductivity of the hanging ear and the surface temperature is not monotonic. The same surface temperature can be obtained when the thermal conductivity is 0.8 and 1.3, and the minimum surface temperature can be obtained when the thermal conductivity is 1.0.

The random grid search method is selected for parameter optimization, with the aim of finding the optimal parameter combination to maximize the temperature of the 8 target surfaces, including the fan motor surface, rear suspension cushion, corrugated pipe rear suspension ear, fuel tank outer surface, ECU surface, left side surface of the rear bumper, the closest point of the fuel pipe to the exhaust pipe, and the center point of the lower surface of the battery pack, to the experimental values.

After obtaining MLP and random forest models, this paper proposes a weighted voting strategy of "output dimension correlation". Firstly, extract 30% from the training set as an independent validation set, and then use a grid search strategy to select MLP weights with a weight range of {0,1} and a step size of 0.05. With the goal of minimizing the MSE of the validation set, the optimal weights for each dimension are determined as shown in the table below:

Table 4.2.1-1: Optimal Weights

Fusion algorithm	Emissivity	Al-Conductivity	Rubber-Conductivity
MLP Weight	0.85	0.20	0.15
Random Forest Weight	0.15	0.80	0.85

Merge the outputs of two models on the test set according to their corresponding weights. This strategy not only retains the dominance of MLP over the emissivity, but also makes full use of the stable estimation of RF for the three thermal conductivities to avoid a single model bias. The following table shows the performance results of two separate models and the ensemble model on the test set:

Table 4.2.1-2: Test Results

MSE / R^2	MLP	RF	Ensemble
Emissivity	0.0021/0.9231	0.0048/0.7815	0.0012/0.9791
Al-Conductivity	26.3592/0.1129	21.9873/0.1635	19.7467/0.1958
Rubber-Conductivity	0.0681/0.1546	0.0401/0.2838	0.0371/0.3042

Overall, the fusion model showed an average improvement of 18.75% and 17.26% in MSE and R^2 com/pared to the best performing individual model in the three output indicators of ear radiation coefficient, exhaust pipe heat shield thermal conductivity, and exhaust ear thermal conductivity, respectively, verifying the effectiveness of the weighted voting strategy. The Intel Xeon 8358 was used for training in terms of computational efficiency, with the MLP model taking a total of 4.5 seconds and the random forest model taking 2.7 seconds. The overall training of the model can be completed within 10 seconds, and the iterative development efficiency is high.

The optimal parameter combination obtained is shown in the following table:

Table 4.2.1-3: Optimal Parameter Combination

Variable	Front suspension	Floor panel	Engine	Exhaust pipe	Heat Shield	Exhaust lifting ear
Emissivity	0.690	0.763	0.522	0.677	0.270	0.948
Thermal conductivity(W/m-K)		/			237.101	1.405

4.2.2. Verification method and result analysis

Verify according to the method in section 4.1.2, set the simulation model according to the parameters in Table 4.2.1-3, and obtain the CFD results as shown in the following table:

Table 4.2.2-1: Simulation Results

Target component temperature(℃)	Experimental value	Simulated value	Absolute error	Relative error

Exhaust lifting ear	74.5	71.2	3.3	4%

The result meets the absolute error requirement of less than ± 5 ℃, and the relative error is also within an acceptable range. Compared to manual simulation results, the absolute error was reduced by 1.9 ℃ and the simulation accuracy was improved by 2.5%. As the number of training samples increases, the accuracy will further improve.

The comparison between manual calibration technology and multivariate integration technology is shown in the following table:

Table 4.2.2-2: Comparison between Multivariate Integration Technology and Manual Calibration Technology

	Absolute error	Relative error	Time consumption for single target optimization	Feasibility of multi-objective optimization
Manual calibration technology	5.2 ℃	7%	288 hours	Low
Multivariate integrated calibration technology	3.3 ℃	4%	10 seconds	High

5 Conclusions and Prospects

5.1 Research findings

- 1. Based on the multi-dimensional integration technology of full-scale automotive climate numerical wind tunnel, a simulation model of automotive heat damage has been successfully constructed. Through reasonable simplification of modeling, grid division, coupling simulation, and benchmarking analysis, it can accurately simulate physical phenomena such as convective heat transfer, heat conduction, and heat radiation involved in automotive heat damage problems.

- 2. Through climate wind tunnel testing and data collection, real and reliable test data were obtained. Scientific calibration methods were used to calibrate the simulation model. After verification, the calibrated simulation model has high accuracy and reliability, which can provide effective analysis methods and design optimization basis for the study of automotive thermal hazards.

- 3. Adopting multivariate integration technology has the advantage of improving simulation accuracy compared to manual calibration, and has significant efficiency advantages in dealing with multivariate and multi-objective problems in engineering.

5.2 Research Prospects

- 1. Further improve the accuracy of the simulation model, consider the mutual influence between more component parameters, in order to more accurately simulate the problem of automobile heat damage.
- 2. Strengthen the integration of diversified integration technology with advanced technologies such as artificial intelligence and machine learning, achieve automatic optimization and rapid prediction of simulation models, and improve research efficiency.
- 3. Expand the research scope and apply this technology to new fields such as battery thermal management and fuel cell thermal damage in new energy vehicles, providing technical support for the development of new energy vehicles.

Acknowledgements

This work was sponsored by the National Key R&D Program of China (Project Number: 2022YFE0208000). The authors would like to thank the China Automotive Technology and Research Center team on the wind tunnel for their support and the colleagues from the vehicle aerodynamics and thermal management department for the assisting discussions.

6 Reference list

[1] Kang Tingting, Li Yantao The impact of extended range vehicle heat damage on battery packs[J]. battery, 2025, 55 (01): 124-128. DOI:10.19535/j.1001-1579.2025.01.020.

[2] Fan Peng, Ma Dehui, Deng Xiang, etc Thermal Management Design and Typical Problem Analysis Application of Extended Range Electric Vehicles[J]. Shanghai Automotive, 2025, (01): 9-14.

[3] Yihu City, Fu Wenqi, Ma Mingjun, etc Study on the Influence of Geothermal Radiation on High Temperature Testing of Whole Vehicles[J]. auto electric, 2024, (12): 81-84.

[4] Liu Chunlei Design and Analysis of Exhaust System for a Certain Vehicle Model Based on CFD Method [D]. Nanchang University, 2023.DOI:10.27232/d.cnki.gnchu.2023.002997.

[5] Sun Xiaogang Thermal Management Analysis of Exhaust System in Extended Range Hybrid Vehicles [J]. Automotive Practical Technology, 2023, 48 (09): 23-28. DOI: 10.16638/j.cnki. 1671-7988.2023.09.005.

[6] Sun Quanhai, Gao Dayi, Chen Chuanzhen, etc Research on Thermal Damage of Hidden Exhaust Duct Vehicle Rear Bumper Skin [C]//China Society of Automotive Engineers, Automotive Aerodynamics Committee of China SAE. Proceedings of the 2022 Annual Conference of the Automotive Aerodynamics Committee of China Society of Automotive Engineers - Thermal Management Sub venue FAW Volkswagen Automotive Co., Ltd; , 2022: 76-80. DOI:10.26914/c.cnkihy.2022.035469.

[7] Yihu City, Huang Yin, Mei Zheng, etc Research on Deviation of Environmental Chamber Test Results Based on Environmental Wind Tunnel [J]. Automotive Practical Technology, 2020, 45 (21): 148-151. DOI: 10.16638/j.cnki. 1671-7988.2020.21.047.

[8] Qin Zhijun Simulation Optimization and Experimental Study on Thermal Damage Protection of Hybrid Electric Vehicles [D]. Northeastern University, 2021 DOI:10.27007/d.cnki.gdbeu.2021.001916.

[9] Ghani A A A S ,Aroussi A ,Rice E .Simulation of road vehicle natural environment in a climatic wind tunnel.[J].Simul. Pr. Theory,2001,8(6-7):359-375.

[10] Song Xin, Li Shuya, Yan Jie, etc Research on the correlation between numerical wind tunnel simulation and open road simulation [J]. Automotive Engineering, 2020, 42 (06): 759-764. DOI: 10.19562/j. cinasae. qcgc. 2020.06.008.

[11] Tao H ,Jinsheng L ,Xianzhong H , et al.Extended Study of Full-Scale Wind Tunnel Test and Simulation Analysis Based on DrivAer Model[J].Proceedings of the Institution of Mechanical Engineers, Part D: Journal of Automobile Engineering,2022,236(10-11):2433-2447.

[12] Ljungskog E ,Sebben S ,Broniewicz A .Inclusion of the physical wind tunnel in vehicle CFD simulations for improved prediction quality[J].Journal of Wind Engineering & Industrial Aerodynamics,2020,197104055-104055.

[13] Engineering - Wind Engineering; New Wind Engineering Data Have Been Reported by Researchers at Chalmers University of Technology (Inclusion of the Physical Wind Tunnel In Vehicle Cfd Simulations for Improved Prediction Quality)[J].Energy Weekly News,2020.

[14] Parsa N ,Abolghasemi H ,Kamkari B .Experimental and numerical investigation of thermal performance enhancement in shell-and-tube latent heat storage

systems: effects of fins, eccentricity, and shell geometry[J].Journal of Energy Storage,2025,128117159-117159.

[15] Guedri K ,Al-Ghamdi S A .Improved Finite Volume Method for Three-Dimensional Radiative Heat Transfer in Complex Enclosures Containing Homogenous and Inhomogeneous Participating Media[J].Heat Transfer Engineering,2018,39(15):1364-1376.

[16] Wang Hongchao, Dan Xizhuang, Yang Zhigang Numerical and Experimental Study on Thermal Management of a Passenger Car Engine Cabin [C]//Proceedings of the 2017 Academic Annual Meeting of the Automotive Aerodynamics Branch of the Chinese Society of Automotive Engineers Tongji University Shanghai Ground Transportation Wind Tunnel Center; ,2017:271-279.

[17] Wang Dan, Xu Junfang, Zhang Yilun, etc The Influence of Front end Module Design on Cooling System of Electric Vehicles [J]. Equipment Manufacturing Technology, 2022, (02): 5-7+17.

[18] Yang Sheng Research on Semi Physical Simulation Test Platform for Automotive Thermal Management System [D]. Tsinghua University, 2004.

[19] Xu Xiang, Wang Yuan, Yu Yilong, etc Numerical simulation and experimental study of the flow field of automobiles in environmental wind tunnels [J]. Automotive Engineering, 2024, 46 (03): 536-545. DOI: 10.19562/j.cinasae. qcgc. 2022.03.018.

[20] Tobias E ,Matthias E ,David K , et al.Snow Contamination of Simplified Automotive Bluff Bodies: A Comparison Between Wind Tunnel Experiments and Numerical Modeling[J].SAE International Journal of Advances and Current Practices in Mobility,2022,4(6):2120-2134.